Semicircular Waveguide-Type Diplexers Used for the Millimeter-Wave Waveguide Transmission System

SADAKUNI SHIMADA, MEMBER, IEEE, AND NOBUO SUZUKI, STUDENT MEMBER, IEEE

***Abstract*—A semicircular waveguide-type diplexer consisting of semicircular hybrids and high-pass filters as a band-splitting filter for millimeter-wave multiplexing–demultiplexing networks has been newly developed. The construction and the operating principles of the diplexer are described; the design method and the experimental results are also discussed. The branching characteristics for a diplexer for dividing the frequency band 43.4–86.8 GHz into two equal parts have proved tolerably flat, with the resulting branching loss amounting to as small as 1.2–1.4 dB. The total length for the experimental model is 1.17 m, which is one-half to one-third shorter than the conventional Michelson interferometer-type diplexer. It is concluded that the semicircular waveguide-type diplexer can be effectively used for millimeter-wave waveguide transmission system.**

I. Introduction

THE Nippon Telegraph and Telephone Public Corporation (NTT) made a field test for the practical application of a millimeter-wave waveguide transmission system [1] in 1972 and 1973. The trial system with two terminal stations and one intermediate repeater station operates over a 22.7-km route.

In this system, using a frequency range of 43–87 GHz and a clock frequency of 403 MBd [a bit-rate of 806 Mb/s with four-phase phase-shift keyed (PSK)], there needs to be 52 channel-dropping filters. The stacking of all these filters in cascade would be quite impracticable. It is proposed, therefore, that the band be split into four groups (*A*, *B*, *C*, and *D*) by means of two kinds of band-splitting filters I and II [2]–[4], as shown in Fig. 1. Each group includes 13 channel-dropping filters under the design requirement that the band spacing between adjacent channels is 810 MHz. The solid-state repeater has an overall front-end noise figure of 11 dB and output of 10.8 dBm at 50 GHz. The size of 13 repeaters are as small as 1043 × 225 × 2100 mm³ [1].

A Michelson interferometer-type diplexer [5] has been proposed for the band-splitting filter I having very broadband properties extending to an octave. However, this diplexer requires considerable space because it is based upon quasi-optical techniques [6].

We have newly developed a semicircular waveguide-type diplexer [7] of small size; one-half to one-third in length in comparison with the Michelson interferometer-type diplexer which can be effectively used as the band-splitting filter I.

Manuscript received April 4, 1973; revised June 14, 1973.
The authors are with the Electrical Communication Laboratories, Nippon Telegraph and Telephone Public Corporation, Yokosuka, Tokyo, Japan.

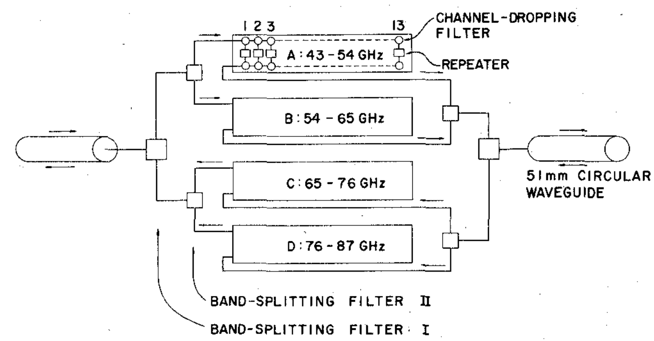

Fig. 1. Multiplexing and demultiplexing network.

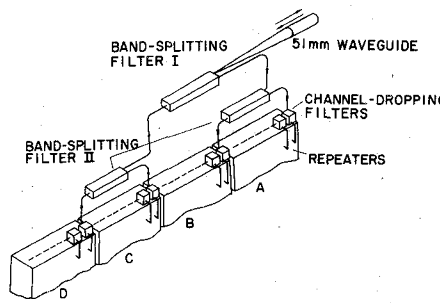

Fig. 2. Filter arrangement.

This facilitates the compact filter arrangement, as sketched in Fig. 2, where a figure-8-type diplexer [8], [9], a rectangular waveguide-type diplexer [10], and a ring-type diplexer [4], [11], [12] already developed are used as the band-splitting filter II for groups *C* and *D*, for groups *A* and *B*, and the channel-dropping filters, respectively.

In the following, the structure, operating principles, and general design method of the semicircular waveguide-type diplexer are first presented. Second, the practical design of 43–87-GHz diplexers is described. Finally, the experimental results are given.

II. Structure and Operating Principles

The semicircular waveguide-type diplexer consists of two hybrid circuits and two cutoff filters with high-pass responses (see Fig. 3). The hybrid is a coupled wave-type 3-dB directional coupler which is composed of two parallel TE_{01} mode semicircular waveguides, coupled to each other by a large number of small circular holes cut in the common plane wall.

The use of many uniformly distributed coupling holes enables one to flatten the coupling versus frequency

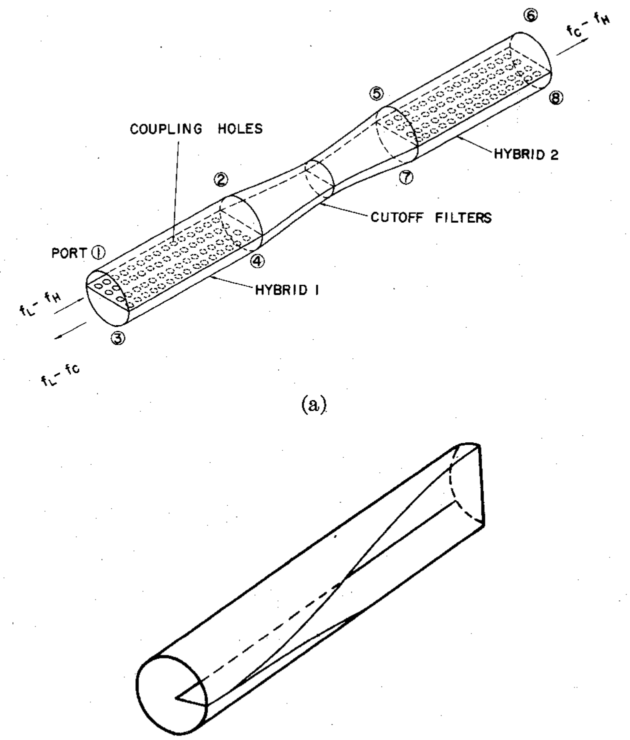

Fig. 3. Semicircular waveguide-type diplexer. (a) Fundamental construction. (b) Circular-to-semicircular mode transducer.

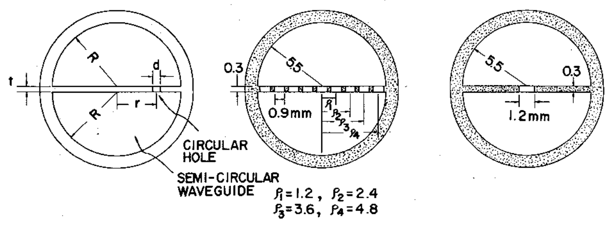

(a) (b) (c)

Fig. 4. Cross-sectional view of semicircular waveguide hybrids.

characteristics, to suppress the excitation of undesired modes, and to shorten the hybrid length.

The operating principles are described in the following. A signal with a frequency band of f_L–f_H (the lowest and highest frequencies of the band, respectively) input at port ① will output from ports ② and ④, approximately equally divided by hybrid 1. Usually the directivity is sufficiently good, and there is little coupling to port ③. The lower band of f_L–f_c (f_c being the cutoff frequency of the cutoff filter) is reflected by the cutoff filters, again passes through hybrid 1 and emerges from port ③. The higher band of f_c–f_H in ports ② and ④ penetrates the cutoff filters and emerges from port ⑧ after being combined with hybrid 2. In this way the frequency band f_L–f_H is split into two bands, f_L–f_c and f_c–f_H.

If the hybrid circuits had an ideal 3-dB coupling over the whole frequency range from f_L–f_H, then no output would appear at ports ① and ⑥. In practice, however, coupling of the hybrid varies with frequency. Therefore, the bands f_L–f_c and f_c–f_H have appreciable coupling to ports ① and ⑥, respectively. The former results in a reflective wave at port ①. The latter is called the residual coupling in this paper. These unwanted couplings cause an increase in the band-splitting loss, referred to as the coupling loss in this paper.

The figure-8-type diplexer is based upon the same operating principles discussed above, but the maximum percentage bandwidth, the ratio of the overall bandwidth to the cutoff frequency, is much narrower than that of the semicircular waveguide-type diplexer, typically 70 percent. The reason is that, in the figure-8 hybrid, the coupling variation with frequency is relatively large because only axial magnetic field contributes to the coupling. Unwanted modes, especially at TE_{31} mode, are excited in the higher frequency region because mode discrimination is caused by only the phase constant difference between the main TE_{01} mode and each unwanted mode [13].

A Japanese fan-type tapered semicircular TE_{01} to circular TE_{01} mode transducer [14], as shown in Fig. 3(b), is used for connecting the semicircular waveguide-type diplexer to the circular waveguide. The similar tapered transducer is also used for connection to the rectangular waveguide.

III. Design Formula

Generally the following conditions must be satisfied in designing the coupled-wave-type hybrid: 1) the phase constants for both waveguides must be equal, and 2) the coupling length to satisfy 3-dB coupling must be determined.

In the case of the semicircular waveguide-type hybrid, condition 1) is automatically satisfied[1] when the two waveguides have an identical inner radius R as shown in Fig. 4. Therefore, we need only consider condition 2).

The amplitude coupling coefficient C_T of a small circular hole with a diameter d located at a radius r from the center of the semicircular waveguide [see Fig. 4 (a)] is approximately given according to Bethe's theory [15] as

$$C_T = C_z + C_r + C_\phi \tag{1}$$

$$C_z = \frac{\chi^2 \lambda_g}{2\pi^2 R^4} \left\{ \frac{J_0(\chi r/R)}{J_0(\chi)} \right\}^2 M_z \eta_m e^{-A_m} \tag{2}$$

$$C_r = \frac{2}{\lambda_g R^2} \left\{ \frac{J_1(\chi r/R)}{J_0(\chi)} \right\}^2 M_r \eta_m e^{-A_m} \tag{3}$$

$$C_\phi = -\frac{2\lambda_g}{\lambda^2 R^2} \left\{ \frac{J_1(\chi r/R)}{J_0(\chi)} \right\}^2 P_\phi \eta_p e^{-A_p} \tag{4}$$

[1] The inner diameter difference between the two semicircular waveguides must be within ±8 and ±25 μm at 43 and 87 GHz, respectively, in order that the residual coupling is kept below −20 dB in a 0-dB coupler with R = 5.5 mm and 480-mm length. This condition can be satisfied by introducing the high precision machining described later.

where

C_z, C_r, C_ϕ amplitude coupling coefficients due to axial and radial magnetic fields (H_z and H_r) and a circumferential electric field (E_ϕ);

λ wavelength in free space;

λ_g guide wavelength for a TE_{01} mode;

χ the first root of $J_1 = 0$ except zero; ($\chi = 3.83171$);

J_0, J_1 the first and second order of Bessel function, respectively [$J_0(\chi) = -0.4028$];

$M_z = M_r = \dfrac{d^3}{6}$ magnetic polarizability;

$P_\phi = \dfrac{d^3}{12}$ electric polarizability;

and where e^{-A_m} and e^{-A_p} are correction factors to evaluate the coupling decrease due to wall thickness t;

$$A_m = \frac{2\pi t}{\lambda_m}\left[1 - \left(\frac{\lambda_m}{\lambda}\right)^2\right]^{1/2}, \qquad \lambda_m = 1.706\, d, \quad \lambda_m < \lambda \tag{5}$$

$$A_p = \frac{2\pi t}{\lambda_p}\left[1 - \left(\frac{\lambda_p}{\lambda}\right)^2\right]^{1/2}, \qquad \lambda_p = 1.306\, d, \quad \lambda_p < \lambda \tag{6}$$

and, moreover, η_m and η_p are other correction factors representing the coupling increase due to resonance effect in the hole;

$$\eta_m = \frac{1}{1 - (\lambda_m/\lambda)^2} \tag{7}$$

$$\eta_p = \frac{1}{1 - (\lambda_p/\lambda)^2}. \tag{8}$$

The coupling holes can be arranged along the axial and radial directions. The number of holes along each direction is represented as N and n, respectively. Fig. 4(b) and (c) shows two examples. The former hybrid has nine holes ($n = 9$) along the radial direction and a large number of holes along the axial direction. It is called a nine-hole-row hybrid. On the other hand, the latter hybrid has only one hole row ($n = 1$) cut along the center axis of the common wall.

The amplitude coupling coefficient per a set of holes on the radial lines C_{Tn} can be easily obtained as is illustrated by the following examples; for the one-hole-row hybrid,

$$C_{T1} = C_z(r = 0) \tag{9}$$

and for the nine-hole-row hybrid,

$$C_{T9} = C_z(r = 0) + 2\left(\sum_\rho C_z + \sum_\rho C_r + \sum_\rho C_\phi\right) \tag{10}$$

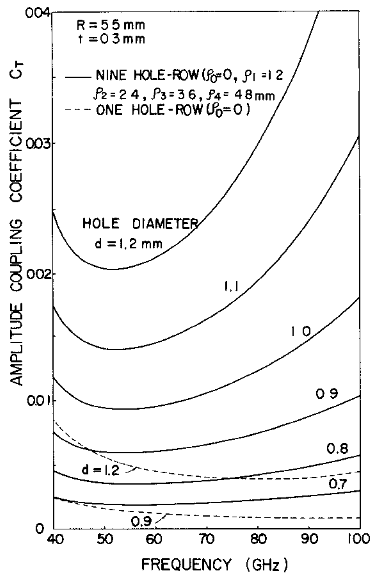

Fig. 5. Calculated coupling coefficient versus frequency.

where

$$\sum_\rho C = \sum C(\rho = \rho_1) + C(\rho = \rho_2) + C(\rho = \rho_3) + C(\rho = \rho_4). \tag{11}$$

Using C_{Tn}, the number of holes along the axial direction N_0 necessary to obtain -3 dB at the frequency f_0 (wavelength λ_0) is given by

$$C_{Tn}(\lambda = \lambda_0) \cdot N_0 = \pi/4. \tag{12}$$

If the center-to-center spacing between the adjacent holes p is constant over the whole coupling section, the coupling length of the 3-dB hybrid L will be

$$L = N_0 p = \pi/4 \cdot p / C_{Tn}(\lambda = \lambda_0). \tag{13}$$

Fig. 5 shows the calculated amplitude coupling coefficients of the one-hole-row and the nine-hole-row couplers when the radius R is 5.5 mm and the wall thickness t is 0.3 mm. Coupling increase in the lower frequency band is mainly due to the contribution of the C_z component, while that in the higher frequency range is governed by the C_r component. When the diameter of the hole d becomes 1 mm or more, the coupling increases abruptly in the higher frequency band because of the resonance effect of the hole.

IV. Design

A. Specification

Four diplexers have been made for the field test [10] with the following specifications:

1) frequency band: 43.395–86. 745 GHz;
2) separating frequency: 65.070 GHz;
3) guard band: 750 MHz;
4) reflection coefficient: below -20 dB (VSWR: below 1.22);

5) residual coupling: below -20 dB.

The separating frequency and the guard band are determined by the cutoff filters. As the former is almost coincident with the cutoff frequency of the cutoff filter f_c, the diameter of the cutoff waveguide section is selected to be 5.619 mm. If the dimension error for the diameter is within ± 5 μm, the deviation from the designed cutoff frequency will be within ∓ 60 MHz.

The temperature variation in the repeater stations, which is expected to be 0°C–40°C (20 ± 20°C), causes expansion or contraction in the cutoff waveguide, resulting in a frequency deviation within ∓ 26 MHz when the waveguide is made of coin silver. Considering these two effects, the separation bandwidth of the cutoff filter f_s expressing sharpness in its frequency response, which is defined as the difference between frequencies where the reflection loss and the transmission loss are 20 dB, should be narrower than 578 MHz. In practice, we have aimed at $f_s \leq 300$ MHz, and obtained the following results [16]:

1) tapered waveguide section: cosine-cubed in shape, 150 mm length;

2) cutoff waveguide section: 5.619-mm ID, 20 mm length;

3) input and output waveguides: 11-mm ID.

Next, the reflection characteristics of the diplexer are discussed. The power level of the pulse echo caused in the multiplexing–demultiplexing networks has been apportioned to be as low as -29 dB according to the pulse-waveform transmission evaluation. The networks include many components such as pressure seals, band-splitting filters, mode transducers, channel-dropping filters, flexible waveguides, and bends. It is almost impossible to adjust the reflection properties by means of stub tuners, etc., in the very broad-band components constructed by the multimode waveguides. For this reason each component must be designed to be well matched.

Lastly, the higher band residual coupling coefficient is related to the transmit–receive interference in the case when the lower and higher frequency bands are transmitted and received, respectively. We have specified this value to be less than -20 dB. In contrast to the above case, the transmit–receive interference in the case that the higher and lower frequency bands are transmitted and received, respectively, gives almost no problem because of the cutoff attenuation of the cutoff filter.

B. Diplexer Using Identical Hybrids

Let us consider first the case of the same hybrid for H_1 and H_2 with a nine-hole-row hybrid [see Fig. 3(a)]. In this case, assume that the maximum and minimum values of C_{Tn} are $C_{\max}$ and $C_{\min}$, respectively. The frequency for which the 3-dB coupling is attained can be chosen so that C_{Tn} is the arithmetic average of $C_{\max}$ and $C_{\min}$, i.e.,

$$C_{Tn}(\lambda = \lambda_0) = (C_{\max} + C_{\min})/2. \qquad (14)$$

We denote $C_{Tn}(\lambda = \lambda_0)$ as C_0. In either case when the

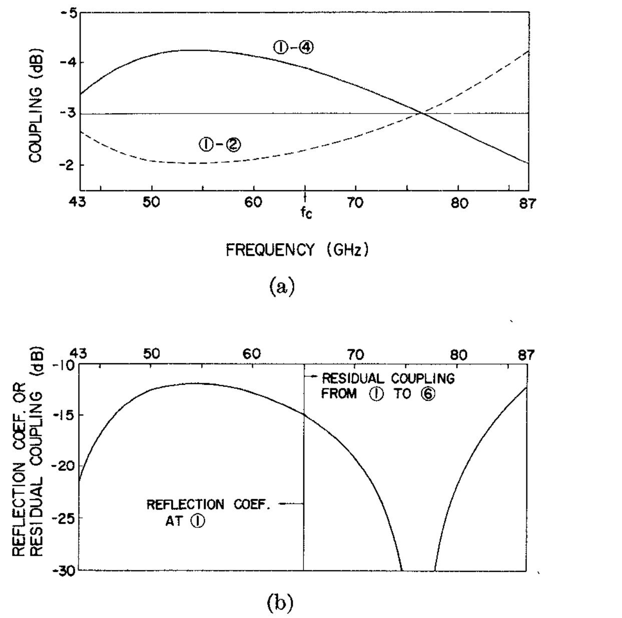

Fig. 6. Calculated properties of a 43.4–86.8-GHz band-splitting filter where hybrids 1 and 2 are the same. (a) Coupling variations with frequency of the hybrid circuit shown in Fig. 4(b). (b) Power reflection coefficient at port ① and residual coupling from ports ① to ⑥.

coupling is large ($C_{Tn} > C_0$) or small ($C_{Tn} < C_0$), the coupling loss is increased. In order for the coupling losses at the maximum C_{Tn} and minimum C_{Tn} to equal each other, it is seen from (14) that

$$C_{\max} - C_0 = C_0 - C_{\min}. \qquad (15)$$

Now, by choosing $d = 0.9$ mm and assuming $f_L = 43.4$ GHz and $f_H = 86.8$ GHz, the coupling characteristic of the 3-dB hybrid with $N_0 = 111$ is shown in Fig. 6. Maximum reflection coefficient at port ① is -12 dB. This value does not satisfy the specification.

C. Diplexer Using Dissimilar Hybrids

Note first that the wave in the lower band is independent of hybrid 2 because it only makes a round trip in hybrid 1. Therefore, hybrid 1 can be designed in such a manner that the coupling deviation in the band f_L–f_c be as small as possible. On the other hand, since the wave in the higher band goes through hybrids 1 and 2, hybrid 2 can be designed in such a manner that the overall coupling characteristics of the cascade connection of both hybrids will be 0 dB. In this case, the coupling deviation in the band f_c–f_H must be designed to be as small as possible. Using this method we can design the hybrid only for half of the full band. Therefore, the usable bandwidth of the branching filter becomes double with respect to that of the conventional method. We describe below the design method in detail.

First, in the lower frequency band of 43.395–65.070 GHz, the number of holes along the axial direction of hybrid H_1 with the structure shown in Fig. 4(b), N_1 is obtained from (12) and (14) as

$$N_1 = 125.$$

TABLE I
MANUFACTURED HYBRIDS

Type	Number of Coupling Holes along Radial Direction	Length (mm)	Number of Coupling Holes along Axial Direction — Hole Diameter (mm) 1.2	1.1	1.0	0.9	0.8	0.7	0.6	Specification
A	Nine hole-row	97.5				62	1	1	1	R = 5.5 mm P = 1.5 t = 0.3 ρ_1 = 1.2 ρ_2 = 2.4 ρ_3 = 3.6 ρ_4 = 4.8
B	"	94.5				63				
C	"	52.5				35				
D	"	33.0				22				
E	One hole-row	102.0	64	1	1	1	1			R = 5.5 mm P = 1.5 t = 0.3
F	"	75.0	50							
G	"	64.5	53							
H	"	45.0	30							

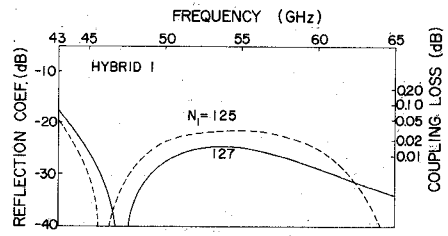

Fig. 7. Power reflection coefficient at port ① and coupling loss from ports ① to ③.

The characteristics of this hybrid are shown in Fig. 7. The dotted line in Fig. 7 shows the reflection coefficient of port ① when ports ② and ④ are totally reflected. This value is less than -21.6 dB and, therefore, satisfies the specification. The coupling loss through ports ①–③ is as small as 0.03 dB.

Next, denote the power coupling coefficients of the hybrids H_1 and H_2 as K_1 and K_2. If

$$K_1 + K_2 = 1 \tag{16}$$

in the higher frequency band of 65.070–86.745 GHz, the coupling loss of ports ①–⑧ is 0 dB. The calculated value of the power coupling coefficient K_1 of the hybrid H_1 and that of K_2 in the ideal hybrid H_2, respectively, are shown in Fig. 8(a). Also shown are the ranges of the residual coupling less than -15 and -20 dB. Therefore, the hybrid whose coupling characteristics are close to the dotted line of Fig. 8(a) is required. Now, using the hybrid H_2 with the structure shown in Fig. 4(c), we obtain K_2 curve (designed) of Fig. 8(a). Where N_2 is 163 that satisfies

$$C_{T9}(\lambda = \lambda_0) \cdot N_1 + C_{T1}(\lambda = \lambda_0) \cdot N_2 = \frac{\pi}{2} \tag{17}$$

at 80 GHz ($\lambda_0 = 3.75$ mm). Here, the fact that importance is placed upon the characteristics near f_c rather than f_H has been taken into consideration. Furthermore, the residual coupling of ports ①–⑥ in the higher-frequency band is shown in Fig. 8(b). According to this, the worst

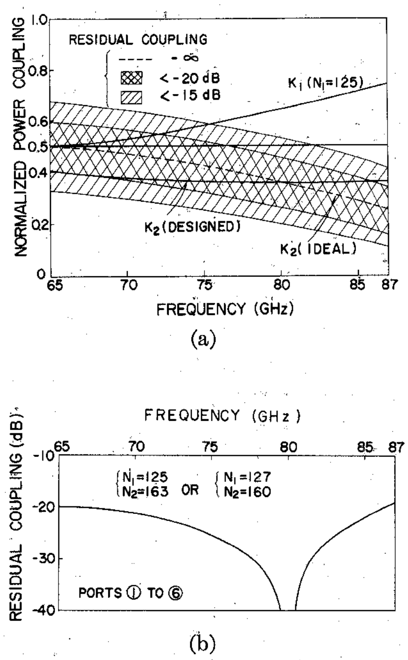

Fig. 8. Designed frequency response of power coupling of hybrid 2 and residual coupling of the filter.

value of the residual coupling is less than -18.9 dB and the coupling loss is less than 0.054 dB.

V. EXPERIMENTAL RESULTS

A. Coupling Characteristics

In order to make the manufacturing simple and the fine adjustment of the length possible, four kinds of coupler shown in Table I were manufactured. Couplers A and E have coupling holes whose diameters become smaller and smaller towards the end of the hole row in order to reduce reflection.

First, the hybrid H_1 is constructed in the order of $A + C + D + D$ (N_1 is about 142.5 with the equivalent diameter 0.9 mm and the total length is 216 mm). The reflection coefficients were measured using the circuit shown in Fig. 9(a). Fig. 9(b) shows the experimental results, which agree with the calculated values shown in Fig. 8(b).

B. Diplexer Characteristics

The length of the hybrid H_2 was chosen to be longer than the previously calculated value in order to mostly reduce the residual coupling near cutoff frequency f_c. However, to avoid the increase of the residual coupling more than -15 dB near 87 GHz, the total length became 267 mm with the composition of $E + F + H + H$.

Fig. 10(a) is a photograph of the complete diplexer. The total length is 1172 mm. Mode filters (semicircular helix waveguide) with lengths 100 mm, 100 mm, and 65 mm are inserted in ports ①, ③, and ⑧, respectively (Fig. 3). Furthermore, circular to semicircular mode transducers are inserted at the input/output ports of the filter. These have electrical characteristics as shown below:

1) length: 150 mm;
2) insertion loss: 0.2 dB;
3) VSWR: 1.12 (the reflection loss less than -25 dB), frequency 43–87 GHz.

Fig. 10 (b) shows the coupler, which was manufactured by the method shown in Fig. 10(c). Two semicircular aluminum mandrels of diameter 11 mm are used. The circular holes are cut in a phosphor–bronze plate of thickness 0.3 mm by a boring machine. Next, the coupling plate is sandwiched between the semicircular mandrels and copper electroforming is carried out. Subsequently, the mandrels are chemically melted and silverplating is formed. Incidentally, the accuracy of the radius of the hybrid is within ± 20 μ.

The cutoff filter is made by a similar method. However, the taper section uses a mandrel whose figure is stepwise shaped by a numerically controlled machine.

The semicircular helix waveguide is made from a circular helix waveguide with the inner diameter 11 mm cut in half and soldered with the flat metallic plate. The loss per 100 mm is 0.06–0.11 dB in the range of 43–87 GHz. This value is $2 \sim 2.5$ times the loss of the semicircular waveguide as shown in Fig. 11 and is half of the loss reported thus far [7].

Finally, the frequency response of the band-splitting filter is shown in Fig. 12 which was measured using a backward-wave oscillator (BWO) sweep generator. As is shown in the figure, the loss in the lower frequency range is 1.2–1.4 dB, and that in higher frequency range is 1.3–1.4 dB. The band-splitting loss of 1.2 dB was obtained from the values in the following table:

hybrid	0.4 dB
cutoff filter	0.1 dB
connecting parts	0.1 dB
semicircular helix waveguide	0.2 dB
mode transducer	0.4 dB

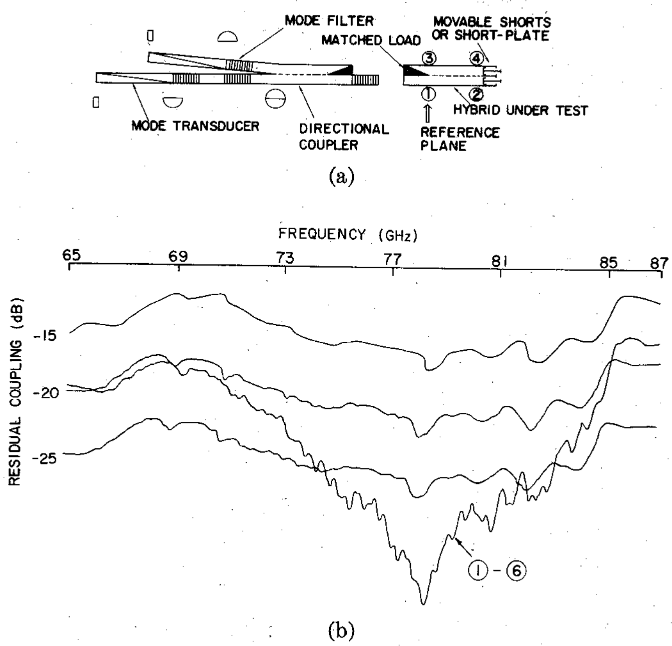

Fig. 9. Evaluation of hybrid properties. (a) Setup for measuring reflection coefficients. (b) Measured residual coupling.

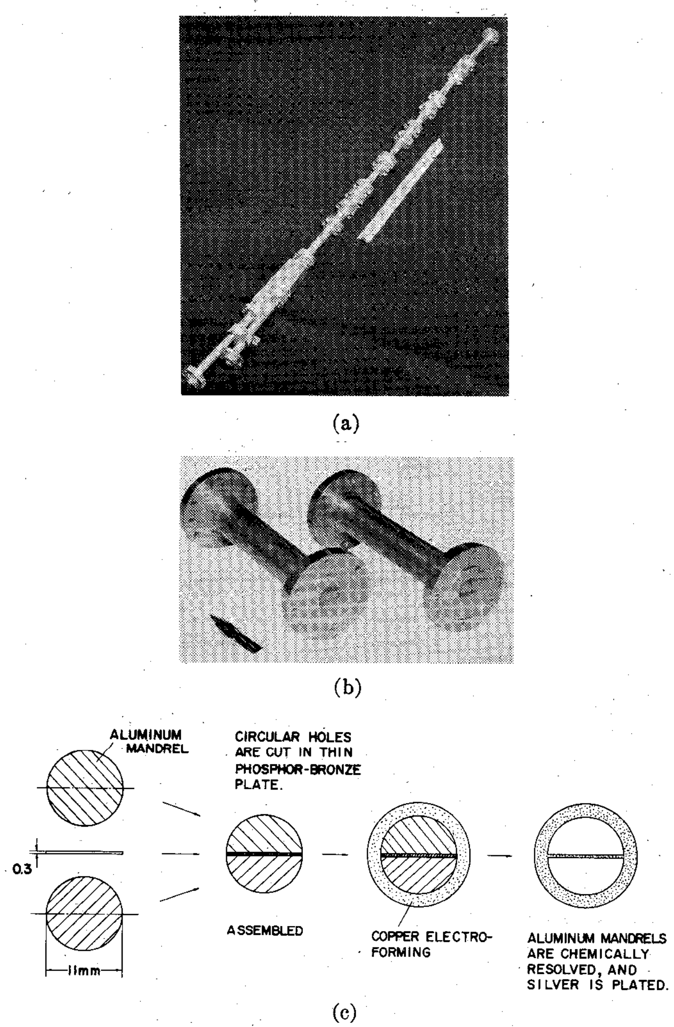

Fig. 10. 43–87-GHz diplexer. (a) Overall view. (b) Part of hybrid 1 (right) and of hybrid 2 (left). (c) Fabrication method of hybrid.

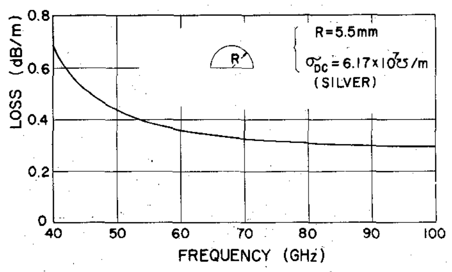

Fig. 11. Theoretical loss of the semicircular waveguide with a radius of 5.5 mm.

Very flat response over the whole frequency range without undesired increase of the loss was obtained. The frequency interval at the 20-dB point of the losses ①–③ and ①–⑧ is 237 MHz, the deviation of f_c is -36 MHz, and the reflection level of the stopband is less than -20 dB. These values satisfy the specification. The residual coupling is -28 dB near 65 GHz without the cutoff filter, but deteriorates to -13.5 dB at most with the cutoff filter. The VSWR of port ① is less than 1.12 (reflection loss -25 dB) over 46–62 GHz and less than 1.22 except for this range.

Incidentally, the VSWR deteriorates near the cutoff frequency f_c. However, it gives no problem because it is in the guard band. The characteristics of port ③ are similar to the characteristics of port ①. The VSWR of port ⑧ is 1.08 (reflection loss -28 dB) at most in the higher frequency range and in almost all frequency ranges, less than 1.07 (reflection loss -30 dB).

VI. Mode Conversions

Mode conversions arising from the semicircular waveguide-type diplexer are due to 1) semicircular hybrid, 2) connecting parts, and 3) offset of the semicircular waveguide.

Let us consider first the semicircular hybrid. Modes arising from the nine-hole-row hybrid differ from the modes from the one-hole-row hybrid. In other words, for the nine-hole-row hybrid the distributed coupling is not only by H_z but also by H_r and E_ϕ. Therefore, the undesired modes coupled with TE_{01} mode are TE_{mn} modes with m zero and even numbers and TM_{mn} modes with m even numbers.

On the other hand, the one-hole-row hybrid couples TE_{0n} modes because its coupling is only by H_z. Now, we try to calculate the mode conversion of the hybrid previously investigated. At a frequency of 80 GHz, the nine-hole-row hybrid produces the undesired TE_{21}, TM_{21}, TM_{41}, and TE_{02} modes. The mode conversion ratio of the TE_{21} and TM_{21} modes is -22 dB and -26 dB, respectively, whereas for the remaining two modes it is less than -30 dB. TE_{02} mode conversion of the one-hole-row hybrid is less than -30 dB.

As seen above, mode conversion losses are small (as low as 0.04 dB) because of the loose coupling between the waveguides of the hybrid. The connecting parts in the diplexer are tilted, facilitiating its connection to other waveguides, as shown in Fig. 10(a). Due to this tilt, undesired modes evolve. Reference [17] shows some ap-

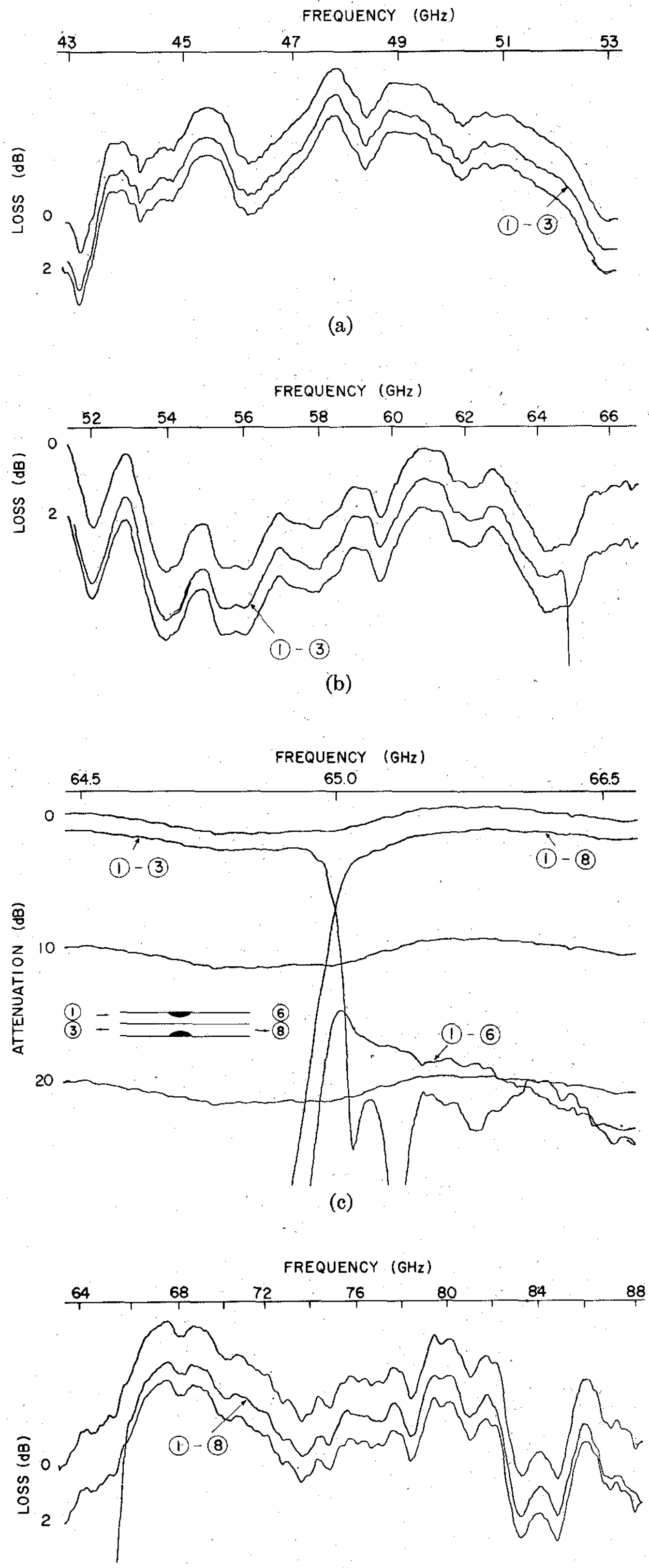

Fig. 12. Measured frequency responses.

proximate calculations for mode conversion of this type. According to these, undesired modes of this case are entirely the same as described for the nine-hole-row hybrid. The tilt angle of the connecting part used in the experiment is 2°51′. In this case the calculated values of mode conversion are −25 dB for the TM_{21} mode and −30 dB for the TE_{02}, TE_{22}, and TE_{21} modes.

Finally, theoretical calculation of the mode conversion due to the small offset of the semicircular waveguide is shown in [18]. Two kinds of offset exist: 1) two semicircular waveguides are offset perpendicular to the flat plane; 2) these are offset parallel to the flat plane. The former produces TE_{0n} modes whereas the latter produces TE_{1n} modes as in a circular waveguide.

Now, assuming that the offset is 0.2 mm for each kind, mode conversions for the TE_{12}, TE_{11}, and TE_{02} modes are −22.2 dB, −28.4 dB, and −30.6 dB, respectively, at 80 GHz. Usually, while modes other than TE_{0n} modes give no problem because of the attenuation by the semicircular helix waveguide, the TE_{02} mode must be given careful attention. Eventually, the mode conversions due to the three items mentioned above are very small and have a negligible effect on the TE_{01} mode.

VII. Conclusions

A wide-band and low-loss diplexer with a loss of 1.2–1.4 dB in the range 43.4–86.8 GHz has been realized. The VSWR is less than 1.22 in the lower frequency band (less than 1.12 in most of 46–62 GHz) and is less than 1.08 in the higher frequency band. The guard band is as low as 240 MHz, but 400 MHz must be allowed when the temperature variation and manufacturing errors are taken into consideration. The total length for the experimental model is 1.17 m which is from one-half to one-third shorter than a Michelson interferometer-type diplexer previously described [5], and the insertion loss is also considerably lower.

At this time, for the purposes of the field test, the multiplexing and demultiplexing networks have been manufactured, one for the repeater station and two for the terminal stations. The overall loss of the system was 8.2–12 dB when the channel dropping filters were partially installed and 9.6–14.9 dB when those were fully installed. An experiment on the complete system with 22.7-km line and repeaters is being planned.

Acknowledgment

The authors wish to thank Dr. M. Shimba and Dr. K. Miyauchi for their invaluable advice, and Dr. R. W. Beatty for his helpful comments. The authors also wish to thank Dr. S. Ishii of the Hitachi Electronics Co., Ltd., for his endeavors in manufacturing diplexers.

References

[1] K. Miyauchi, "W-40G millimeter-wave waveguide transmission systems," in *Proc. Nat. Conv. Inst. Electron. Commun. Eng. Japan*, 1972.

[2] S. Shimada, I. Ohtomo, and N. Suzuki, "Millimeter-wave branching filter system for 806 Mb/s transmission experiments," *Trans. Inst. Electron. Commun. Eng. Japan*, vol. 54-B, pp. 396–403, July 1971.

[3] K. Miyauchi, S. Kita, S. Shimada, and N. Sushi, "Design and performance of an experimental 400MB-4PSK guided millimeter-wave transmission system," in *Proc. 1970 Inst. Elec. Eng. Conf. Trunk Telecommunications by Guided Waves*, pp. 21–26, Sept. 1970.

[4] S. Shimada, I. Ohtomo, and K. Ohi, "Ring type channel-dropping filter for a guided millimeter-wave communication system," in *Proc. 1970 Inst. Elec. Eng. Conf. Trunk Telecommunications by Guided Waves*, pp. 222–227, Sept. 1970.

[5] E. A. J. Marcatili and D. L. Bisbee, "Band-splitting filter," *Bell Syst. Tech. J.*, vol. 40, pp. 197–212, Jan. 1961.

[6] S. Shimada, N. Suzuki, and I. Ohtomo, "Millimeter-wave branching filter system for PCM transmission experiments," *Elec. Commun. Tech. J.*, Nippon Telegraph and Telephone Public Corp., Japan, vol. 18, pp. 769–780, Nov. 1970.

[7] N. Suzuki, S. Shimada, T. Nunotani, and I. Nakagawa, "Semicircular waveguide type band-splitting filter for millimeter waves," *Trans. Inst. Electron. Commun. Eng. Japan*, vol. 54-B, pp. 839–846, Dec. 1971.

[8] S. Shimada and N. Suzuki, "A new hybrid circuit for circular TE_{01} mode band-splitting filter at millimeter wavelengths," *Rev. Elec. Commun. Lab.*, Nippon Telegraph and Telephone Public Corp., Japan, vol. 16, pp. 805–824, Sept.–Oct. 1968.

[9] S. Shimada, N. Suzuki, and I. Ootomo, "A new millimeter-wave band-splitting filter using figure-8 hybrids," in *IEEE G-MTT 1969 Int. Symp. Dig.*, pp. 232–237, May 1969.

[10] S. Shimada, N. Suzuki, H. Hirotani, and K. Toriyama, "Rectangular waveguide band-splitting filter for a millimeter wave communication system," *Trans. Inst. Electron. Commun. Eng. Japan*, vol. 54-B, pp. 694–695, Oct. 1971.

[11] I. Ohtomo and S. Shimada, "A channel-dropping filter using ring resonators for the millimeter wave communication system," *Trans. Inst. Electron. Commun. Eng. Japan*, vol. 52-B, pp. 265–272, Mar. 1969.

[12] ——, "Channel dropping filters using ring resonators for a millimeter-wave communication system," *Rev. Elec. Commun. Lab.*, Nippon Telegraph and Telephone Public Corp., Japan, vol. 19, pp. 87–98, Jan.–Feb. 1971.

[13] S. Shimada and T. Matsuoka, "TE_{01} mode circular waveguide hybrid for millimeter wave band-splitting filter," *Trans. Inst. Electron. Commun. Eng. Japan*, vol. 51-B, pp. 357–364, Aug. 1968.

[14] K. Toriyama, H. Hirotani, and N. Suzuki, "A tapered mode transducer for a millimeter-wave communication system," in *Proc. Nat. Conv. Inst. Electron. Commun. Eng. Japan*, no. 811, 1972.

[15] H. A. Bethe, "Theory of diffraction by small holes," *Phys. Rev.*, vol. 66, pp. 163–182, Oct. 1944.

[16] N. Suzuki and S. Shimada, "Cosine type cutoff filter for millimeter waves," *Trans. Inst. Electron. Commun. Eng. Japan*, vol. 52-B, pp. 768–775, Dec. 1969.

[17] N. Kumagai and G. Matsuo, "Reflection and mode conversion of TE_{01} wave caused by slight tilt in semi-circular waveguide," *Trans. Inst. Electron. Commun. Eng. Japan*, vol. 46, pp. 1126–1127, Aug. 1963.

[18] K. Hashimoto, "Mode conversion in a slightly off-set TE_{01} mode semi-circular waveguide," *Trans. Inst. Electron. Commun. Eng. Japan*, vol. 56-B, pp. 269–270, June 1973.